Proceedings World Geothermal Congress 2010
Bali, Indonesia, 25-29 April 2010

Rock Properties of North-Eastern Tasmania: Implications for EGS Development

Hilary K.H. Goh, Michael Roach and Anya Reading

CODES, University of Tasmania, Private Bag126, Hobart, Tasmania 7000, Australia

hilarygoh@gmail.com, hilary.goh@kuthenergy.com

Keywords: rock properties, geothermal, EGS, thermal conductivity, Tasmania

ABSTRACT

The potential of the Lower Paleozoic basement rocks of north-east Tasmania as a target for Enhanced Geothermal System (EGS) development was assessed by a combination of detailed petrophysical and geochemical measurements and one dimensional modeling. The basement rocks in this area consist of an Ordovician to Devonian turbiditic sequence called the Mathinna Group that has been intruded by Devonian granites. The potential of the Mathinna Group rocks to act as thermal insulators was assessed in this study together with the contributions of enhanced heat production from the granitic bodies.

Laboratory measurements of petrophysical, geochemical and thermal rock properties were used to create one-dimensional thermal models of the upper crust. Density, porosity, magnetic susceptibility, sonic velocity and electrical resistivity were measured using standard equipment and laboratory techniques. New inexpensive techniques were developed and refined to measure thermal conductivity, heat capacity and to determine the elemental abundances of K, U and Th using a hand-held gamma ray spectrometer.

Mathinna Group sandstones have the highest thermal conductivity values (~4.4 W/mK) and shales the lowest (~2.7 W/mK). Granites have intermediate thermal conductivities (~3.5 W/mK). The Mathinna Group rocks all have very low heat production but four granite bodies sampled all have high heat production with values in excess of >7 uW/m^3 and a maximum value of 22.7 uW/m^3 for a sample from the Royal George pluton.

Modeling suggest that fine-grained Mathinna Group sedimentary packages have the potential to act as basement insulators to increase temperature gradients in the presence of high heat producing granites and hence represents potential targets for EGS. The presence of a widespread low thermal conductivity cover sequence over the Lower Paleozoic basement units further enhances the potential for EGS exploration in eastern Tasmania.

1. INTRODUCTION

Enhanced Geothermal Systems are a new field of geological exploration requiring new types of data and knowledge to develop improved heat flow models of the crust.

It is projected that Enhanced Geothermal System power plants will be able to provide base load power equivalent to a coal-fired power station (Barbier 2002). Also, as a sustainable source of energy Enhanced Geothermal Systems have the potential to provide large amounts of base load electricity which is currently beyond the capability of other renewable technologies i.e. wind, solar and hydro power generation (Fridleifsson et al. 2008).

This project investigated the petrophysical, geochemical and thermal characteristics of the Mathinna Group metasediments and the Devonian granites of north eastern Tasmania. The primary aims were 1) To evaluate the rock properties and heat production potential of Lower Paleozoic basement rocks of north eastern Tasmania which are the Ordovician- Devonian Mathinna Group (turbiditic sandstones, shales, siltstones and mudstones) and the Devonian granites, and 2) To assess the potential of Mathinna Group lithologies as insulators for any heat producing granites.

One model for EGS is that the Mathinna Group sequences may act as an insulating layer due to their low thermal conductivity values, hence leading to high geothermal gradients in the presence of high heat flows from deep sources or upper crustal high heat producing granites. This project provides new numerical data to enable this assessment. Data were acquired from a suite of 90 samples using five standard and five developmental methods. All experiments took place at laboratories at the Earth Sciences building, University of Tasmania, Hobart, Australia.

A total of nine diamond drill holes have been sampled for this project. All metasedimentary samples are from the Silurian to Devonian part of the Mathinna Group. And four Devonian granites were sampled: Poimena, Gipps Creek, Royal George and Coles Bay granites.

This project focused on method development. It utilised new devices, methods or modifications to existing methods to record electrical resistivity, thermal conductivity, heat capacity and K, U, Th elemental abundances. Bulk rock properties were measured on diamond drill core available from the Mineral Resources Tasmania Core Library in Rosy, Tasmania. The effect of fractures, joints, veins, anisotropy, mineralogy and water saturation on rock properties were not considered in this project as these factors require more specific and detailed studies. Non-destructive methods were preferred so the samples could be tested on multiple methods.

This paper will only focus on the results of the experiments and not the one-dimensional modeling or method development for new techniques.

2. REGIONAL GEOLOGY OF TASMANIA

The study area was located in the north eastern part of Tasmania, Australia in the East Tasmanian Terrane (Figure 1; Seymour, Green and Calver, 2007). It ranges from the towns of Coles Bay in the south east, Scottsdale in the northwest, Avoca in the southwest and St Helens in the east.

The lower Paleozoic geology of Tasmania can be roughly divided into the East Tasmanian Terrane (~1/3 of

Tasmania) and the West Tasmanian Terrane. The boundary between the terranes is concealed by the upper Paleozoic rocks of the Tasmanian Basin and recent studies suggest the boundary is marked by faults of the Tiers Lineament (Burrett & Martin 1989; Leaman 1994; Powell et al. 1993).

The basement of both terranes incorporate rocks up to late Devonian and are overlain by the Permian to Triassic Parmeener Group; flat lying fluvial and glacial sediments which are ~1.3km thick in some places. Jurassic dolerite intrudes sill-like into the Parmeener as well as covering a large proportion of the surface in the eastern half of Tasmania (Figure 1) (Burrett & Martin 1989).

2.1 East Tasmanian Terrane

The East Tasmania Terrane (ETT) has a simpler geology compared to the more complex West Tasmanian Terrane. The Ordovician to Devonian Mathinna Group comprises the basement and a significant proportion of the terrane. Devonian granites, of both S and I types, intruded passively upwards into the Mathinna resulting in some contact metamorphism. After a period of erosion the Parmeener Group sediments blanketed the surface and these in turn were intruded and overlain by extensive volumes of Jurassic dolerite.

2.1.1 Mathinna Group

The Mathinna Group (a.k.a. Mathinna Beds) metasediments are Ordovician to Devonian turbidite sequences that extend from the Furneaux Group of islands in the north down to Port Arthur in south (Figure 1). The environment of deposition was most likely a continental slope with density currents producing turbidite successions (Burrett & Martin 1989). The Mathinna Group metasediments range in age from the Early Ordovician (488.3Ma) to Early Devonian (407.0 Ma) (Bottrill et al. 1998; Burrett & Martin 1989; Powell et al. 1993). Early Devonian granites intrude into the Mathinna at various depths (McClenaghan 2006).

The detailed stratigraphy is poorly understood due to a lack of readily correlated units and biostratigraphic control (very few fossils) (Burrett & Martin 1989). Overall individual beds range from centimetres to metres thick with some sandstone units up to 4m in thickness (Powell et al. 1993). Sandstones and siltstones are usually massive with thinly bedded muds and shales. Younging of the beds is from west to east. The beds have been folded and deformed in a NW-NE trending strike with upright east facing overturned folds with low grade metamorphism (Burrett & Martin 1989). It is difficult to determine the total thickness of the sequence as the top is an erosional contact with the Parmeener Group and no drilling has yet penetrated the base (Bottrill et al. 1998; Powell et al. 1993). It is estimated to be at least 7 km thick in some places, particularly in the south, with a minimum thickness of 1 km (Powell et al. 1993).

Originally the Mathinna Group was broken into two loose age units, Ordovician and the Silurian-Devonian. There are no know contacts between the two age units and it was hypothesised that there may be an unconformity or fault which marks the boundary (Burrett & Martin 1989; Powell et al. 1993). The Ordovician sequence has a smaller outcrop area than the Silurian to Devonian beds (Burrett & Martin 1989). The Ordovician sequence is dominated by massive medium to coarse siltstone and fine mudstone units interrupted with some sandstones. Coarse sandstones are present but these are rare (Burrett & Martin 1989). Beds are about 2m thick (Burrett & Martin 1989; Powell et al. 1993).

The Silurian-Devonian beds crop out to the north east of Scamander (Figure 1). This sequence is dominated by sandy unit and contains alternating beds of poorly sorted siltstones, mudstones and graded sandstones (Burrett & Martin 1989). Laminations are also present in some of the fine grained beds as well as sole markings and slumping. Full Bouma divisons are seen in this unit (Burrett & Martin 1989).

More recently the Mathinna Group has been broken into 4 possible formations (Bottrill et al. 1998; Powell et al. 1993). The oldest formation is called the Stony Head Sandstone which is ~1km thick and dominated by fine to medium quartz sandstones with some mudstones (Bottrill et al. 1998; Powell et al. 1993). This is followed by the 1-2km thick Turquoise Bluff Slate in which the lower half is massive muds and the upper half mudstones combined with fine siltstone and sandstone beds (Bottrill et al. 1998; Powell et al. 1993). The Bellingham Formation conformably overlies the Turquoise Bluff Slate, is ~2km thick and made up of mud dominated classic quartzose turbidites. (Bottrill et al. 1998; Powell et al. 1993). The last formation is the Sidling Sandstone made up of hardened quartz sandstone and which is greater than 2km in thickness (Bottrill et al. 1998; Powell et al. 1993).

This new classification only confidently differentiates the four units west of the town Bridport, all turbidite sequences to the east are undifferentiated (Powell et al. 1993). The samples collected in this project come from the eastern region and therefore have been grouped according to lithology rather than formation.

2.1.2 Devonian Granites

The Devonian granites range in age from 395 ±1.5 to 348 ± 10 Ma and intrude upwards into the Mathinna Group with some contact metamorphism (Burrett & Martin 1989). Erosion has exposed them at the surface and they outcrop in the north east of Tasmania and along the east coast (Figure 1). Intrusion is inferred to have been passive with magma intruding dilation zones or stoping the Mathinna Group rocks (Burrett & Martin 1989; McClenaghan 2006). The intrusions range from granodiorites to pink (alkali-feldspar) granites with the majority of plutons described as adamellites or granodiorites (McClenaghan 2006). Textures range from porphyritic to very coarse grains (McClenaghan 2006).

There appear to be four main batholiths in the East Tasmanian Terrane along with other individual intrusives (Figure 2) (McClenaghan 2006). These are the Scottsdale, Ben Lomond, Blue Tier and Eddystone batholiths. The Ben Lomond batholith appears to be made up of lesser disconnected bodies (Burrett & Martin 1989; McClenaghan 2006). Four granites were sampled for this project: Royal George, Gipps Creek, Coles Bay and Poimena.

The Coles Bay granite does not appear to be apart of any batholith (Figure 2) and is an I type granite/adamellite from the Freycinet Suite (Burrett & Martin 1989; McClenaghan 2006). This granite has a distinctive pink colouration, though some parts are highly felsic, with both prophyritic and equigranular textures throughout the body. Grain sizes range from medium to very large crystals.

The Poimena granite belongs to the Poimena Suite which is from the Blue Tier batholith (McClenaghan 2006). This is an I type granite/adamellite with abundant large K-feldspar crystals. It has an equigranular texture with medium to coarse grains (Burrett & Martin 1989; McClenaghan 2006).

Both the Royal George and Gipps Creek granites are from the Royal George Suite which is apart of the Ben Lomond batholith (McClenaghan 2006). In some articles the Royal George granite is classed as an individual pluton though it does have compositional similarities with the Ben Lomond Batholith (Burrett & Martin 1989; McClenaghan 2006). Both the Royal George and Gipps Creek are S type granites with large alkali feldspars. The Royal George granite predominantly has very coarse grains and phaneritic texture. The Gipps Creek granite is also coarse grained with a prophyritic texture (Burrett & Martin 1989; McClenaghan 2006).

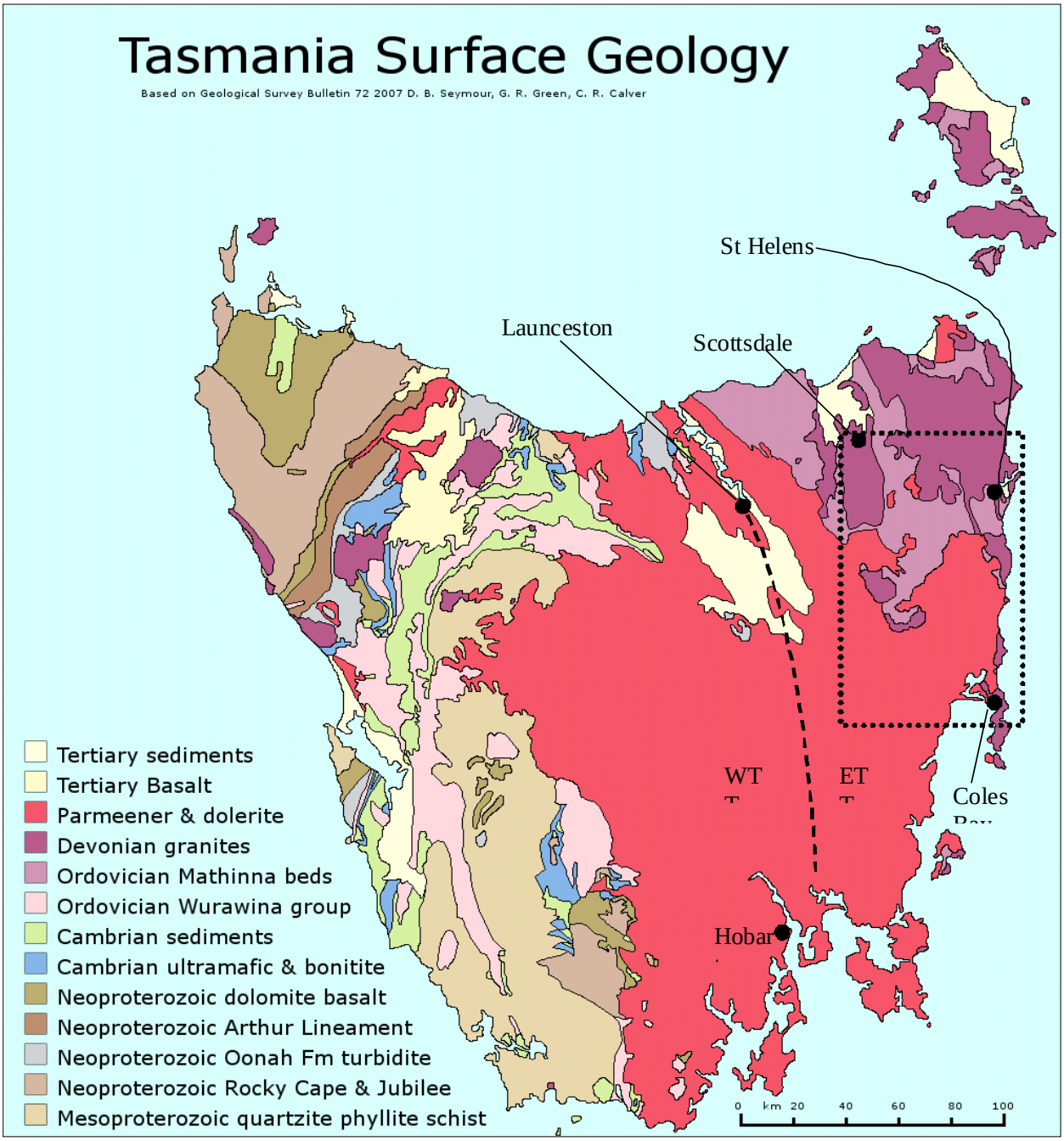

Figure 1: Study area (black dotted box) overlain onto surface geology of Tasmania. Black dots are populated areas. The black line is the inferred boundary between the East (ETT) and West Tasmanian Terranes (WTT). Based on Geological Survey Bulletin 72 2007 by D.B. Seymour, G.R. Green, and C.R. Calver.

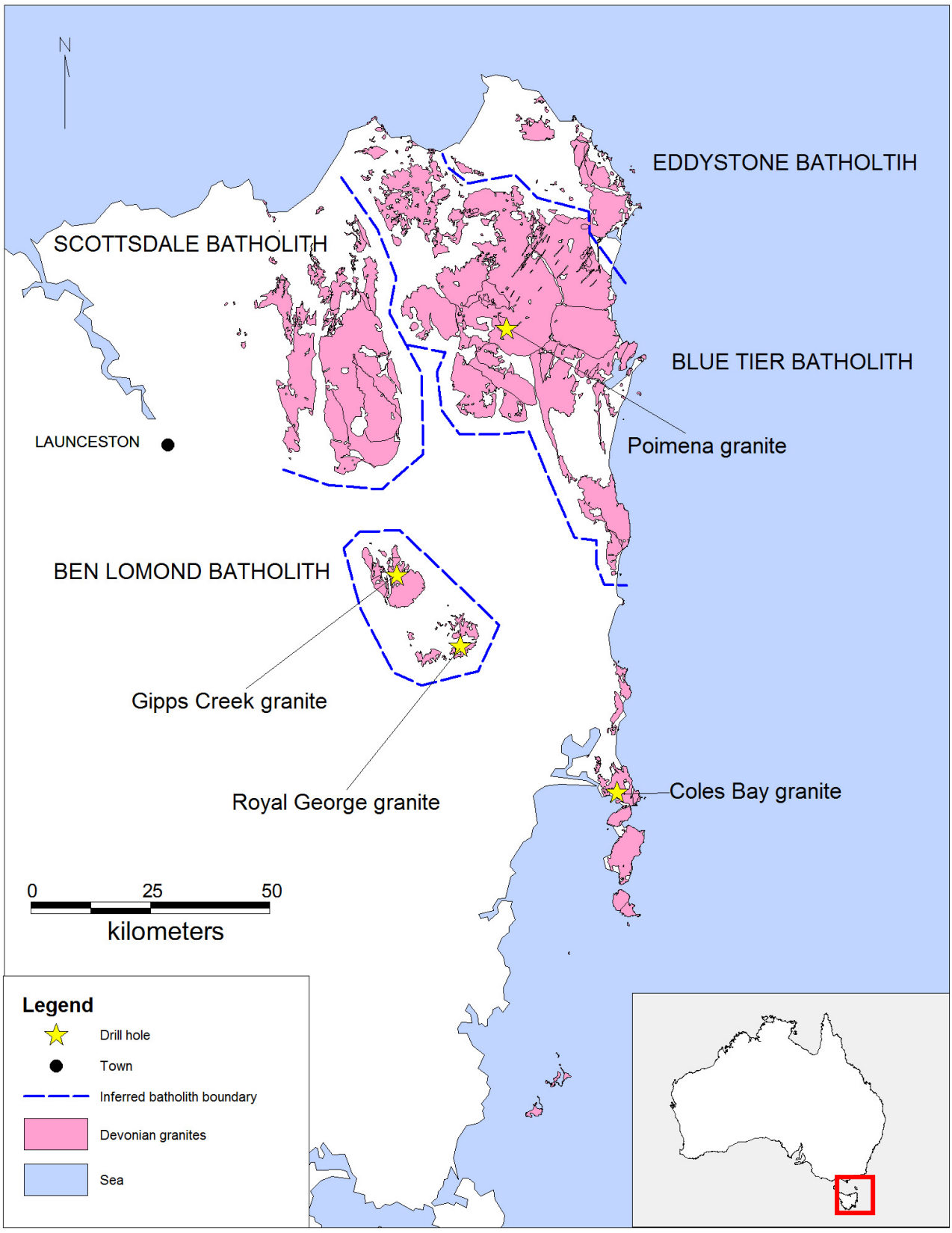

Figure 2: Devonian granite outcrops in north eastern Tasmania. Dashed lines indicate extent of batholiths. Drill holes indicate location of individual granites sampled for this project.

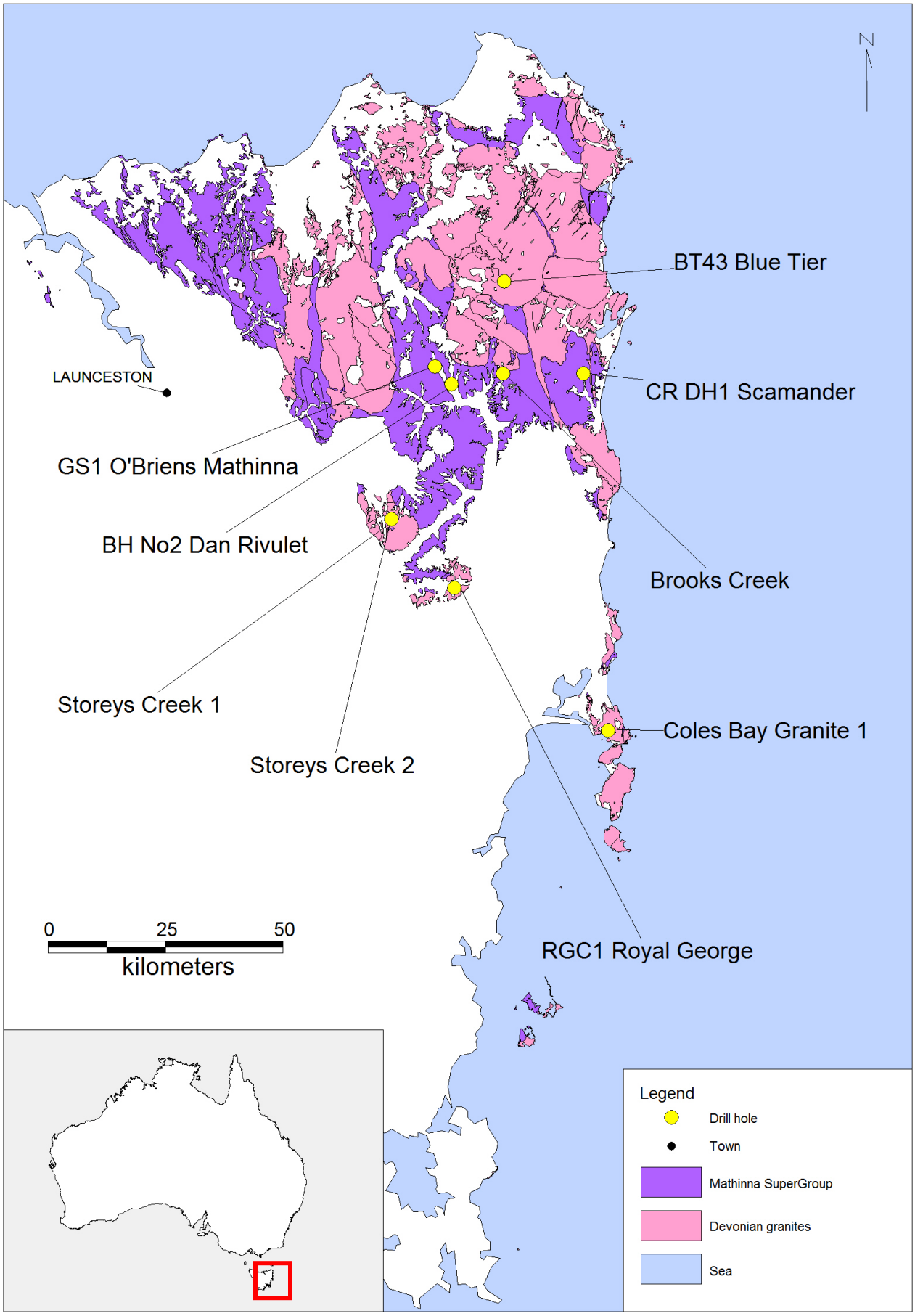

Figure 3: Location of sampled drill holes in north eastern Tasmania and outcrops of the Mathinna Group sediments and Devonian granites.

3. SAMPLING

Sampling was restricted to north eastern Tasmania due to the outcropping Mathinna Group sediments and high heat generating granites (from radiometric data) in this area. GIS and radiometric maps were used to help select the desired drill holes to sample Mathinna sediments and granites (Figure 3).

A total of 92 fully cored competent samples (45-50cm diameter) were taken from 9 holes (Table 1). The Dans Rivulet hole was oversampled to ensure representative sampling of the lithological variability. Samples were cut to ~8cm in length for all tests but thermal conductivity which was performed at the end (Figure 4). For this experiment samples were cut to ~2cm in length and the ends were polished smooth (Figure 5). Off cuts when cutting samples to 8cm were used for the geochemical tests.

Table 1: Number of samples taken from each hole and their respective lithology

Drill Hole Name	No. samples	Geological unit
Dans Rivulet BH No.2	30	Mathinna Group
Brooks Creek	18	Mathinna Group
GS1 O'Briens Mathinna	5	Mathinna Group
CR DH1 Scamander	8	Mathinna Group
BT43 Blue Tier	6	Poimena granite
Storeys Creek 1 & 2	4	Gipps Creek granite
Coles Bay granite	14	Coles Bay granite
RGC1	7	Royal George granite

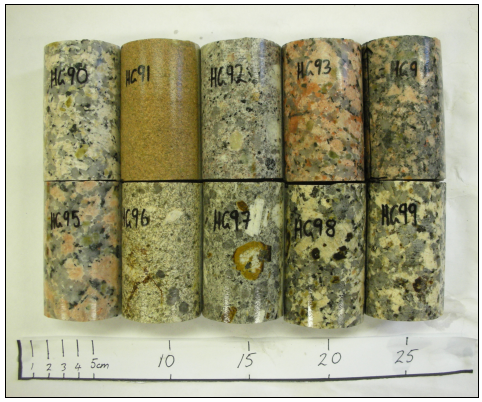

Figure 4: Selection of Devonian granite samples cut to ~8cm in length.

Figure 5: Selection of samples cut to ~2cm in length and with both ends polished.

4. EXPERIMENTAL METHODS

Experiments for magnetic susceptibility, density, porosity, sonic velocity and X-ray fluorescence used comparatively standard techniques. Five methods were developmental requiring calibration and validation of results before use: electrical resistivity, thermal conductivity, heat capacity, Gamma Ray Spectroscopy and LA-ICP-MS. Calibration and validation of these techniques will be detailed in a future paper and technical questions can be directed to Dr Michael Roach.

4.1 Petrophysical Methods

Only electrical resistivity uses a non-standard technique and is detailed here. Magnetic susceptibility, density, porosity and sonic velocity measurements involved applications of standard methods

4.1.1 Magnetic Susceptibility

Magnetic susceptibility measurements were taken first as this required no preparation of the samples. Measurements were taken with a KT-9 Kappameter, in $x10^{-3}$ SI Units, and an average value was calculated from three readings.

4.1.2 Density and Porosity

Samples had been sitting in core trays for a considerable period and it was presumed they had lost a lot of their water content. Therefore dry density preparation and measurements were undertaken first and then saturation and wet density measurements. After cutting core to ~8cm length samples, batches of 30 were put in an oven for 72 hours at 50ºC to drive out any remaining fluids. After dry density measurements samples were placed in water filled buckets for at least 72 hours to hydrate for wet density measurements (vacuum saturation was not conducted).

Porosity was calculated from the dry and wet density results.

4.1.3 Sonic Velocity

A CNS Electronics PUNDIT was used to measure sonic (P wave) transit through the sample, Δt (in microseconds). Sonic velocity was determined from the time it takes for a seismic wave to pass through a sample of a given length (Telford, Geldart & Sheriff 1990). A sonic gel was applied to ensure good contact between the sample ends and transponders and all measurements were taken on saturated samples. Two different transponders were used depending on the diameter of the samples. The smaller transponder for NQ core runs at 82 KHz and the larger for HQ core runs at 54 KHz. A check piece, with a Δt of 26 microseconds, was used to calibrate the device after every five samples.

4.1.4 Electrical Resistivity

Electrical resistivity is an intrinsic property that describes how strongly a material resists the flow of electrical current due to an applied voltage. For unmineralised rocks the electrical resistivity is primarily determined by, the porosity and permeability of the sample, the degree of water saturation, and the electrical properties of the electrolyte. A material is a conductor if the values are $<10^{-5}$Ohm m, a semi conductor between 10^{-5}Ohm m to 10^{7}Ohm m and an insulator $>10^{7}$Ohm m (Telford, Geldart & Sheriff 1990). Electrical resistivity is scale dependent and measurements on lab samples record the properties of the in-tact rock but do not take into account electrical conduction through joints, fractures or along bedding surfaces. For this reason

laboratory measurements usually overestimate the in-situ bulk electrical resistivity.

All samples were saturated with Hobart tap water and surface dried when tested on this device. For this experiment the samples had flat ends as they were clamped between two horizontally secured plexiglass tube to create an electrical contact (Figure 6). Each tube was filled with a sponge that was saturated in slightly saline water (30g NaCl in 14 L of Hobart tap water). All resistivity measurements were conducted using a four electrode system. Two platinum potential electrodes were positioned immediately adjacent to the sample ends to record the voltage drop across the sample and two current electrodes were placed at the opposite ends of the tubes to record the resistance of the voltmeter. The system was energised using a laboratory signal generator operating at a frequency of 30Hz. Total current through the circuit was recorded by measurement of the potential across the 200K Ohm resistor in series with the sample and measurement system. The Fluke 196C Scopemeter (RMS voltage) displayed all signals and measured voltages (Vp and Vi). These two measurements, which only took a few minutes, were required to calculate the electrical resistivity (Ohm m) of the sample (Equations 1-3).

The majority of samples were very resistive and current density through the samples was very low. Normally with low to moderate resistivity samples, it is usually assumed that almost all the current passes through the sample and little or no current passes though the voltmeter in parallel with the sample. Unfortunately, due to the highly resistive nature of many of the samples this assumption was not valid and conventional formulae used to calculate laboratory resistivity had to be modified to incorporate the internal resistance of the Fluke Scopemeter (107 Ohms).

Three equations were needed to calculate electrical resistivity and the total resistance of the circuit,

$$Rr = \frac{Vp*Rm}{Rm*(Vi/Rs)-Vp} \quad (1)$$

$$Rt = \frac{Rs*Vp}{Vi} \quad (2)$$

$$\rho = \frac{Rr*a}{L} \quad (3)$$

where *Vp, Vi, Rm, Rs, Rr, Rt, a, L,* ρ are the voltage across the sample, the voltage across the series resistor, resistance of the voltmeter, (assumed $1x10^7\Omega$ from the scope meter manual), resistance of the ~200KΩ resistor, (measured 220.5kΩ), resistance of the rock, total resistance of sample and ~200KΩ resistor, cross sectional area of the sample, length of the sample and the resistivity of the sample.

4.2 Geochemical Methods

The elemental abundances (K, U and Th) were used to calculate heat generation for heat flow models. XRF and ICP-MS are standard and precise methods for determining elemental composition but are expensive and require some preparation of rock samples i.e. crushing. Gamma Ray Spectroscopy (GRS) was chosen as a quicker and simpler alternative method and samples could be saved for other testing methods. GRS in a laboratory requires shielding and correction due to background contamination of the spectra from the surrounding concrete and calibration of results with conventional analyses. A small group of representative samples were analysed using XRF and LA-ICP-MS to validate the GRS results.

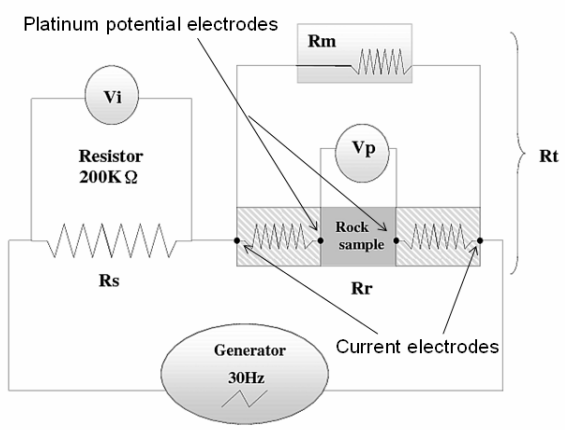

Figure 6: Circuit diagram for electrical resistivity experiment. Black dots represent electrodes.

4.2.1 GRS and Heat Production

Estimation of elemental abundances from GRS spectra required a significant amount of method development since the instrument (GR-130) was used in a lab instead of in the field. The GR-130 was used in the lab as a cheap, simple and quick way to measure the K, U and Th elemental abundances of a large batch of samples, in this case ~90. Using a gamma ray detector in a lab requires no preparation other then cutting all samples to a standard size. This was a cheaper method than XRF and LA-ICP-MS especially for geothermal exploration where only the bulk content of elements and not the rock structure are important.

The Exploranium GR-130G (BGO crystal) was a portable gamma ray spectrometer that records the gamma rays emitted from a sample it was placed next to, usually a rock outcrop. Gamma rays (γ rays) are pure electromagnetic radiation which are emitted during nuclear disintegration (Telford, Geldart & Sheriff 1990). The GR-130 records a gamma ray that was converted to a light photon by a Bismuth Germinate ($Bi_4Ge_3O_{12}$) crystal, the intensity of the light pulse was proportional to the energy of the gamma ray. Naturally occurring gamma ray emitters produce gamma rays with characteristic energies i.e. Potassium has a main peak with an energy of ~1.4 MeV. The detector has 256 channels and records energies between 0-3 MeV. It can therefore discriminate the relative proportion of different radionucleides (Telford, Geldart & Sheriff 1990). For a gamma ray spectrometer the intensity of gamma radiation is influenced by both the elemental composition of the rock and the geometry. The GR-130 spectrometer was calibrated to estimate elemental abundances assessing a half-space source. In this case the system required the calibration to account for the limited (8cm core) source geometry. Compton Scattering has to be taken into account when converting the spectra to elemental concentrations. This scattering occurs when gamma rays collide with electrons and lose energy (Adams & Gasparini 1970). Compton Scattering is manifest in gamma ray spectra as an increasing background value with decreasing energy.

As buildings can emit K, U and Th gamma rays a lead castle was created to prevent these rays reaching the spectrometer during measurement (Adams & Gasparini 1970). The lead castle has an average thickness of ~5-8cm (2-3 inches) and is enclosed in a steel shell (see Figure

5.11). A lead brick of ~5cm (2 inches) is used to cover the entrance during measurement.

Saturated samples (at ~8cm length) were surface dried and the sample plus the GR-130 were placed into a tray that slid into the middle of the lead castle and the lead brick placed over the entrance. A couple of sponges were used to hold the sample in place and it was positioned with the core axis in line with the GR-130 axis. Maintenance of a standard geometric arrangement of the sample and detector is important for ensuring the accuracy and precision of estimates of elemental abundance.

Measurements were run for an hour (3600 seconds) for every sample. This was to ensure an adequate number of gamma rays were detected for very low emitters i.e. sandstones since the accuracy of the results is in part determined by the counting statistics. A Caesium standard (C^{137}), which is apart of the GR-130 kit, was used to stabilise the GR-130 between every measurement. This was to stop any drift (due to temperature changes) occurring in successive measurements (Adams & Gasparini 1970). Background measurements, also for an hour, were taken at the start of sample batches (~6-7 a day).

Only three elements are of interest in these spectra, Potassium (peak at 1.46 MeV), Thorium (peak at 2.62 MeV) and Uranium (peak at 1.76 MeV). Caesium has an energy ~ 0.66 MeV (Telford, Geldart & Sheriff 1990). Spectra were converted into spreadsheet files for analysis. Background spectra were stripped from each sample spectra using a method specified by Minty, Luyendyk & Brodie (1997). The total gamma ray values for each element was estimated from the spectrum by summation of the channels corresponding to the appropriate energies K (channels 114-131), U (channels 138-155) and Th (channels 201-234) (IAEA 1991).

Due to Compton Scattering the Th contributions to the U counts and the contributions from U to the K counts have to be removed by the process of 'stripping' (Minty, Luyendyk & Brodie 1997). Calibration of the gamma ray results with chemical analyses and knowledge of the sample density enables generation of coefficients to convert gamma count rates to elemental abundances. The difference between the wet and dry densities are so small that they don't affect the final results.

After final elemental abundances had been calculated they were used to calculate the average heat generation for each sample (see Equations 4-7) (Beardsmore & Cull 2001).

$$K\ hp = (K\% * Wd * 1000) * 0.0035 \quad (4)$$

where *K hp, K% , Wd* are potassium heat production, K% from sample and the dry mass of sample. 0.0035 (μW/kg element) relative heat generation of K in typical crustal rocks

$$U\ hp = (U\ ppm * Wd * 1000) * 96.7 \quad (5)$$

where *U hp, U ppm, Wd* and uranium heat production, U ppm from sample, ($1x10^{-6}$) and the dry mass of sample. 96.7 (μW/kg element) relative heat generation of U in typical crustal rocks

$$Th\ hp = (Th\ ppm * Wd * 1000) * 26.3 \quad (6)$$

where *Th hp, Th ppm Wd* are thorium heat production, Th ppm from sample, ($1x10^{-6}$) and the dry density of sample. 26.3 (μW/kg element) relative heat generation of Th in typical crustal rocks

$$Total\ HP = K\ hp + U\ hp + Th\ hp \quad (7)$$

where *Total HP* is the total heat production of the sample in ($\mu W/m^3$)

4.3 Thermal Methods

Thermal properties relate to the quantity and ease to which heat may move though a material. Both these methods were developmental.

4.3.1 Thermal Conductivity

Thermal conductivity refers to how easily or quickly heat may move through a material. A Portable Electronic Divided Bar (PEDB) was purchased from Hot Dry Rocks Ltd. Temperature measurements from this device are used to calculate thermal conductivity (Equations 8-12).

All samples were saturated for at least 42 hours before any measurements were taken. Samples were cut to ~2 cm thickness and the ends polished perpendicular to the core axis to ensure good contact with the brass plates. The brass plates have a diameter of 50mm and core diameters ranged in size from ~31-50mm.

The PEDB works by measuring the change in temperature (ΔT) across a cylindrical sample using thermocouples as a hot plate induces heat flow downwards through the sample towards to a cold plate. The bar is arranged vertically and is made up of a hot plate at the top, upper brass plate, the rock sample in the middle, lower brass plate and cold plate contained within the case. The brass plates have low thermal conductivity polycarbonate discs inserted into the middle. A clamp is screwed downwards to secure the sample and vaseline is used on the ends of the sample to ensure good contact with the brass plates. Fluid is used to control the temperature of the hot and cold plates. Two thermocouples are inserted into each brass plate and the known thermal conductivity of the plates are compared to the unknown thermal conductivity of the rock sample. These four thermocouples are plugged into channels on a data logger using Channels 1-4. Heat is induced in a downward direction to ensure heat flow in the sample was not a result of convection (Beardsmore & Cull 2001). Foam pads were placed around the sample to minimise heat loss from the side. The hot plate temperature was set to ~29°C and the cold plate to ~11°C and the PEDB was allowed to warm up for about half and hour. It should be noted that these are data logger temperatures as the digital displays on the device were not working properly. Room temperature was ~21-25°C.

The samples were placed upside down to mimic heat flowing to the surface and clamped down firmly. Temperature measurements from the thermocouples are used to calculate a delta T (ΔT) value and three of these values were recorded for each sample. The first measurement ran for 600 seconds to allow the sample to equilibrate and the next two are 300 seconds each. The last 30 seconds of each measurement are averaged to give three ΔT values. From these ΔT values three thermal conductivities are calculated and then all three are averaged together to give one overall thermal conductivity of the sample. The stated errors of the results are stipulated by the manufacturer depending upon the ΔT value. A correction was applied in the calculations to account for the different diameters (Table 2).

Due to time constraints, the homogenous nature of the samples and the good repeatability of results only one 2cm sample was cut from the original 8cm core for the majority of the samples.

Table 2: Calibration constants used in the calculations as stated by manufacturer

Calibration constants	
A =	0.5986
B =	-86.164
C =	6849.8
D (25.4mm) =	-356
D (37mm) =	-396.323
D (48mm) =	-364.041
D (60mm) =	-309.092

The following equations are specified by the manufacturer to be used with the PEDB to calculate thermal conductivity (Hot Dry Rocks Ltd).

$$\Delta T = \frac{(T_2 - T_3)}{(T_1 - T_2) + (T_3 - T_4)} \quad (8)$$

where ΔT T_1 T_2 T_3 T_4 are the Delta T calculation, temperature from thermocouple inserted in upper part of the hot brass plate, lower part of the hot brass plate, upper part of the cold brass plate and the temperature from thermocouple inserted in lower part of the cold brass plate

$$Sa = \pi (d/2)^2 \quad (9)$$

where Sa, πd are the surface area, 3.147 and the diameter.

$$Slope = A*d^2 + B*d + C \quad (10)$$

Slope/Diameter constants, A,B,C (see Table 2)

$$R/A = \Delta T*Slope + D \quad (11)$$

where R/a, D are the resistance over area and the diameter of the sample, (Table 2)

$$\lambda = 1x10^6* L /((R/a)*Sa) \quad (12)$$

where λ ,L and the thermal conductivity and length of rock sample.

It should be noted that the pressure applied to the sample affects the ΔT value. The more pressure applied results in a lower ΔT value and a higher thermal conductivity. Therefore the sample should be clamped down firmly until the sample does not move (but not so much that you crush softer samples).

4.3.2 Heat Capacity

Heat capacity is the amount of heat that a given material may hold for a specific increase with temperature (Equation 13) (Zumdahl 2000). No rock calorimeter was available at UTAS therefore we created our own. A simple thermos was purchased from an adventure shop and turned into a calorimeter.

The data logger, software and an extra thermocouple from the thermal conductivity experiment were used to record water temperatures inside a thermos. A hole was bored into the side of the thermos just below the rim so that a thermocouple could be inserted and taped against the inside. The hole was filled with glue to stop any escape of water or heat. The end of the thermocouple was located halfway down the thermos to record an average water temperature. A magnetic stirrer was also used to ensure an even distribution of water temperature throughout the thermos and a plastic stand was used to hold the sample above the magnetic stirrer. An electric scale with a precision of 0.1g was used to measure the weights of the water and rock sample.

Samples were dried in an oven for 72 hours at just under 90ºC. After drying the temperature was turned down to 80ºC for measurements. Samples were weighed on the electric scale (M_s) and placed back in the oven. It should be noted that the digital reading of oven temperature was higher than the actual temperature and a 110ºC lab thermometer was placed inside to ensure the right temperature was being reached. Initial samples temperatures are taken from this thermometer (T_d). A thermocouple could not be placed inside as the door of the oven would not close.

Cold water was put into the calorimeter between each measurement to bring it to room temperature and to remove any remaining heat. The lab was automatically air condition and had a low room temperature, ~15ºC. About 300-305 g of water (M_w) was placed into the calorimeter to cover the samples, ~360g were needed for the smaller samples. The calorimeter was left to equilibrate for about 5-10 minutes and then an initial water temperature was recorded from the thermocouple inside the calorimeter (T_1). When ready, a sample was taken from the oven and placed in the calorimeter and the lid screwed on. Equilibration usually took between 800-1200 seconds and final water temperature was than taken (T_2). These five measurements and the heat capacity of water, 4.18J/(g°C), are used to calculate the heat capacity of the sample (Gunn et al. 2005; Zumdahl 2000).

$$HC_r = \frac{M_w * HC_w (T_2 - T_1)}{M_s (T_d - T_2)} \quad (13)$$

where M_w M_s HC_w T_1 T_2 T_d are the mass of water, mass of rock sample, heat capacity of water, (4.18J/(g°C)), initial water temperature in the calorimeter, final water temperature in the calorimeter and the temperature of the sample in the oven.

5. ROCK PROPERTY RESULTS

A summary of all rock properties has been put together and can be found at the end of this paper (Table 3). These results are for bulk properties only and do not take into account the degree of water saturation, anisotropy, jointing, fractures, veining or mineralisation.

Mathinna Group samples are separated into three lithologies; sandstones, siltstones and mudstones, and shales. These groupings are based on grain size and the shales were separated from the siltstones and mudstones due to their different sedimentary structure (very thin lamination). The granite samples from the four plutons are grouped together. A total of 89 (58 sediment and 31 igneous) samples were tested by all methods (Table 4). Three sediment samples are not included; one was destroyed during cutting and the other two were test pieces for the divided bar.

5.1 Magnetic Susceptibility

Sandstones show little variability when three high outliers are excluded from the sample population (Table 5). The silty sediments (siltstones, mudstones and shales) have

higher magnetic susceptibilities and the granites have the lowest with also low variability. There is a small difference between the Mathinna Group lithologies though not enough to be mappable on a regional scale. Magnetic susceptibility has a standard error of ± $0.001x10^{-3}$ for all measurements (calculated from the precision in measurement stated in the Kapameter manual).

Table 4: Number of samples for each lithology. Granites are grouped according to plutonic source.

	Lithology	Number of samples
Mathinna Group	**Total**	**58**
	Sandstones	24
	Siltstones and mudstones	16
	Shales	18
Devonian granites	**Total**	**31**
	Poimena	6
	Gipps Creek	4
	Coles Bay	14
	Royal George	7

Table 5: Magnetic susceptibility by lithology, x10-3

	Lithology	n	Mean	Median	SD	Min	Max
Mathinna Group	Sandstone	24	**2.1**	0.05	5.68	0.01	18.33
	Sandstone*	21	**0.06**	0.04	0.07	0.01	0.33
	Siltstone and mudstone	16	**0.4**	0.18	0.42	0.09	1.51
	Shale	18	**0.16**	0.16	0.02	0.10	0.19
Devonian granite		31	**0.03**	0.03	0.04	0.01	0.23

5.2 Density

There was little variation between dry and wet density due to the low porosity of the samples (Table 6). The silty sediments have a higher density than the sandstones and the granites have the lowest density. This difference between the highest and lowest value was noticeable, ~0.3 g/cm^3.

Table 6: Density by lithology, g/cm^3

			Dry density			Wet Density		
	Lithology	n	Mean	Median	SD	Mean	Median	SD
Mathinna Group	Sandstone	24	**2.68**	2.69	0.12	**2.67**	2.68	0.13
	Sandstone*	23	**2.69**	2.68	0.03	**2.69**	2.68	0.03
	Siltstone and mudstone	16	**2.76**	2.76	0.02	**2.76**	2.76	0.02
	Shale	18	**2.77**	2.77	0.02	**2.76**	2.76	0.02
Devonian granite		31	**2.58**	2.58	0.02	**2.60**	2.60	0.01

5.3 Porosity

All samples except for two outliers have a porosity below 2% excluding three outliers greater than 2% (Table 7). Granites have a lower porosity than the sediments. Low porosities are expected for the Mathinna Group due to minor metamorphism of the sedimentary units.

5.4 Sonic Velocity

The majority of the shales have lower sonic velocities compared to the granites, sandstones and siltstones (Table 8). There is a ~1 km/s difference between the shales and other lithologies which is potentially a geophysically mappable difference at a regional scale provided that the shaly rocks occur in large enough volumes.

Table 7: Porosity by lithology, %

	Lithology	n	Mean	Median	SD	Min	Max
Mathinna Group	Sandstone	24	**1.23**	0.35	4.02	0.07	20.04
	Sandstone*	23	**0.41**	0.24	0.33	0.07	1.29
	Siltstone and mudstone	16	**0.56**	0.47	0.46	0.07	1.63
	Shale	18	**0.90**	0.57	0.86	0.39	4.07
	Shale*	17	**0.70**	0.57	0.35	0.39	1.70
Devonian granite		31	**0.56**	0.46	0.33	0.14	1.46

N= number of samples, SD= standard deviation, *excluding outliers

Table 8: Sonic Velocity by lithology, km/s

	Lithology	n	Mean	Median	SD	Min	Max
Mathinna Group	Sandstone	24	**5.25**	5.50	0.70	2.74	5.79
	Sandstone*	23	**5.35**	5.51	0.46	3.92	5.79
	Siltstone and mudstone	16	**5.18**	5.18	0.65	3.79	6.70
	Shale	18	**4.29**	4.28	0.52	3.45	5.23
Devonian granite		31	**5.49**	5.54	0.25	4.91	5.89

N= number of samples, SD= standard deviation, *excluding one weathered outlier

5.5 Electrical Resistivity

This property was highly variable for all lithologies and the mean values are strongly influenced by outliers (Table 9). In this case the median values provides a more reasonable indication of the in-tact resistivity. These laboratory results are scale dependent and overestimate the *in situ* bulk rock resistivities. They do not take into account the discontinuities in *in situ* rocks such as fractures that are conduits for fluid.

Table 9: Electrical resistivity, Ωm, x10^4

	Lithology	n	Mean	Median	SD	Min	Max
Mathinna Group	Sandstone	24	30.2	**1.2**	89.9	0.057	336.61
	Siltstone and mudstone	16	5.9	**1.3**	15.1	0.026	59.14
	Shale	18	1.8	**1.7**	1.5	0.040	6.55
Devonian granite		31	1.7	**1.3**	2.5	0.054	10.80

N= number of samples, SD= standard deviation

5.6 Heat Production

Granite samples have the highest gamma ray counts overall. Sandstones have gamma counts as low as the background. One sample from the Royal George granite had a very high gamma ray count and was analysed using XRF and LA-ICP-MS. Uranium values for the Mathinna Group are very low (less than ~2ppm) when compared to the granites (> 20 ppm) (Table 10). Thorium values from the shales and siltstones exceed those from the Poimena and Royal George granites. Potassium values are slightly lower for the sediments then the granites. All the sediments have a low heat generation, < 2 uW/m^3. The Royal George granite has the highest uranium and heat generation values with an average of 10.51 µW/m^3 with a maximum of 10.75 µW/m^3. Gipps Creek is ~1 uW/m^3 higher than the Poimena and Coles Bay granites. It appears that the S type granites have a higher average heat generation then I types.

5.7 Heat Capacity

Heat capacity was the least variable of all the rock properties measured in this project. There was very little variation between lithologies, ~0.1 J/gK, from the minimum to maximum value those it does appear that it increases

with decreasing grain size in the Mathinna Group (Table 11).

Table 10: Average U, Th and K elemental abundances for various lithologies from GRS (Incorporates XRF and LA-ICP-MS values for 19 samples used in the calibration). *one sample (HG81) is excluded due to very high anomalous Thorium result.

Lithological group	n	U (ppm)	Th (ppm)	K (%)	A ($\mu W/m^3$)
Mathinna Group (total)	**58**	**1.45**	**13.65**	**2.58**	**1.61** ± 0.03
Sandstone	24	1.22	10.36	1.66	1.20 ± 0.03
Siltstones and mudstones	16	2.07	13.99	3.06	1.87 ± 0.05
Shales	18	1.18	17.74	3.38	1.93 ± 0.04
Devonian granites (total)	**30**	**24.16**	**24.82**	**4.05**	**8.13** ± 0.23
Poimena (I)	6	23.45	13.43	3.69	7.17 ± 0.28
Gipps Creek (S)	3*	18.86	45.62	4.13	8.23 ± 0.41
Coles Bay (I)	14	19.76	29.18	4.16	7.33 ± 0.17
Royal George (S)	7	35.85	16.95	4.11	10.51 ± 0.24

n= number of samples, A= average heat generation, I= I type granite, S= S type granite

Table 11: Heat capacity by lithology, J/gK

	Lithology	n	Mean	Median	SD	Min	Max
Mathinna Group	Sandstone	24	**0.63**	0.63	0.02	0.59	0.69
	Siltstone and mudstone	16	**0.65**	0.65	0.02	0.63	0.69
	Shale	18	**0.66**	0.66	0.02	0.61	0.69
Devonian granite		31	**0.64**	0.64	0.02	0.60	0.68

N= number of samples, SD= standard deviation

5.8 Thermal Conductivity

There was a strong relationship between lithology and thermal conductivity (Figure 7). There was ~ 1W/mK difference in the mean values between the three Mathinna Group lithologies and thermal conductivity decreases with grain size. The majority of sandstones samples had a high thermal conductivity between 4.2 -5.4 W/mK but values as low as 2.2 W/mK. This very low thermal conductivity sandstone can be excluded as it was possibly a shale or siltstone not a sandstone. The siltstones had a lower variability than the sandstones or shales with a mean value of ~3.3 W/mK. One siltstone sample had a very high thermal conductivity (5.13W/mK) as it contained many quartz veins that can possibly channel more heat than usual. Shales had the lowest average thermal conductivity of about 2.7 W/mK and a variability greater than the siltstones and mudstones but not the sandstones. Granites had a low variability in thermal conductivity, 3.0-3.8 W/mK, compared to the high variability from the Mathinna Group samples, 1.44-5.26 W/mK (Table 12). For each Mathinna Group lithology the majority of thermal conductivities were grouped into particular ranges, with siltstones and mudstones overlapping the shale and sandstone ranges. Thermal conductivity ranges increase from the finer grained laminated shales, 1.9-3.2 W/mK, up to siltstones and mudstones, 2.8-4.2 W/mK and finally to the high conductivity sandstones, 4.2-5.4 W/mK. The granites also had a range similar to the siltstones and sit between the majority of shale and sandstone values. In the field where there are no granites present it may be possible to determine different Mathinna Group lithologies based on thermal conductivities.

Four samples broke during cutting and were glued back together. Only one of these, HG18 which was a shale, had a higher thermal conductivity compared to others of the same lithology and was excluded from the average value for shales (Table 12).

Table 12: Thermal conductivity by lithology, W/mK

	Lithology	n	Mean	Median	SD	Min	Max
Mathinna Group	Sandstone	24	**4.38 ± 0.21**	4.72	0.87	2.18	5.26
	Sandstone*	23	**4.48 ± 0.22**	4.76	0.74	2.66	5.26
	Siltstone and mudstone	16	**3.44 ± 0.15**	3.38	0.64	2.71	5.13
	Siltstone and mudstone*	15	**3.33 ± 0.14**	3.32	0.47	2.71	4.14
	Shale	18	**2.71 ± 0.10**	2.59	0.68	1.44	4.05
	Shale*	16	**2.70 ± 0.10**	2.59	0.54	1.99	3.88
Devonian granite		31	**3.48 ± 0.15**	3.50	0.20	3.04	3.86

N= number of samples, SD= standard deviation, *excluding outliers

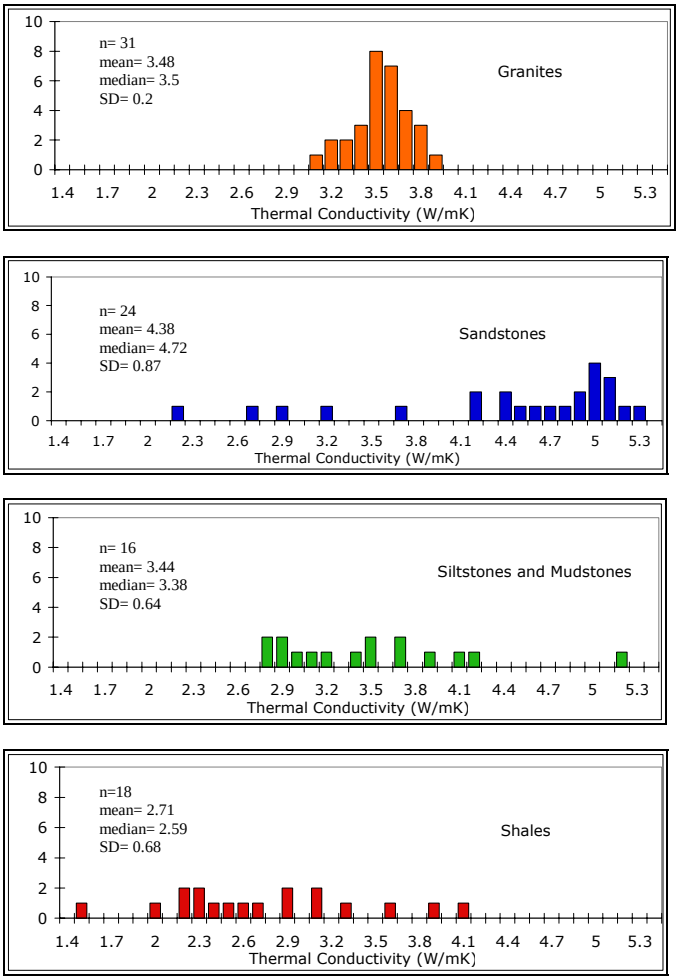

Figure 7: Distribution of thermal conductivity by lithology, including all outliers.

6. DISCUSSION

Overall the Devonian granites have a lower variability in rock properties then the Mathinna Group. Results from this project are for bulk rock properties only, especially for electrical resistivity and thermal conductivity. These two properties are scale sensitive and results differ between hand specimens and outcrops (Telford, Geldart & Sheriff

1990). Thermal conductivity will be underestimated in hand specimens as the role of water advection was not taken into account. Electrical resistivity will be overestimated by sample measurement due to conduction through fluids in fractures. Factors which may affect all the rock properties and are not considered here are; fractures, veins and joints, degree of saturation and mineralization.

There appeared to be no strong relationship between lithology and porosity, electrical resistivity or heat capacity though there was a reasonable but weak relationship with density and magnetic susceptibility (heat capacity did not show any correlation with other rock properties or lithology and is not further discussed in this chapter). Therefore variations in these properties are not useful for pinpointing favourable lithologies using large scale geophysical surveys i.e. magnetic or resistivity surveys. However there were strong lithological relationships with thermal conductivity, sonic velocity and the geochemical data.

There was a weak relationship between magnetic susceptibility, lithology and thermal conductivity, the silty sediments have lower thermal conductivities and higher magnetic susceptibilities while the sandstones have higher thermal conductivities and lower magnetic susceptibilities. The differences between the Mathinna Group lithologies are at a scale too small to be useful for any regional mapping.

Likewise for the density measurements there was a small difference between the Mathinna Group and the Devonian granites densities, ~0.30g/cm^3. Within the Mathinna Group the siltstones, mudstones and shales have a slightly higher density, ~2.77g/cm^3, than the sandstones, ~2.69g/cm^3, but this difference would only be apparent in a gravity survey if large coherent volumes of rock with these properties were located next to each other. There was a small trend between density, sonic velocity and thermal conductivity but these scales are also to small to be useful. The higher density silty Mathinna Group had lower sonic velocity and higher densities with lower thermal conductivities.

Porosities for both the Mathinna Group and the Devonian granites are below 2%. Normally an increase in thermal conductivity occurs with decreasing porosity, particular for sedimentary rocks (Beardsmore & Cull 2001; Popov et al. 2003). This was not seen in the Mathinna Group samples and was most likely due to very low porosities from the low grade metamorphism of the beds compacting pore spaces. Recent studies have also concluded that there was no relationship between low porosities and thermal conductivities (Surma & Geraud 2003) . There appeared to be no trends between lithology and electrical resistivity, sonic velocity and porosity. However if lithology is ignored there is a trend of decreasing electrical resistivity with increasing porosity. Sonic velocity was expected to increase with decreasing porosity according to mixing laws but this did not occur (Beardsmore & Cull 2001; Telford, Geldart & Sheriff 1990).

There are weak or no relationships between thermal conductivity, magnetic susceptibility, density or porosity and this was the same for electrical resistivity. Electrical resistivity was expected to decrease with decreasing thermal conductivity but the results from this project do not support this (Popov et al. 2003). This was also due to the low porosities of both the Mathinna Group and Devonian granites leading to similar volumes of water in the pores. Water was the controlling factor for resistivity values in many rocks (Telford, Geldart & Sheriff 1990).

From the geochemical data it was evident that there was a relationship between K, U and Th content and lithology. Uranium values from the Devonan granites (18-35 U ppm) are much higher then those for the Mathinna Group rocks (1-2 U ppm). Shales, siltstones and mudstones have higher K, U, Th contents then the sandstones. Average K, U and Th values for the Mathinna Group and Devonian granites are similar to those reported by Schmus, 1995.

Most heat generation and surface heat flow values for Australia are from South Australia because of the many geothermal exploration projects taking place due to a predicted high heat flow anomaly in the central to southern part of the state (Matthews & Beardsmore 2007). South Australian values are mentioned here to provide a comparison between Tasmania and South Australia's heat production potential.

The Mathinna Group had a slightly lower heat generation value, <2 μW/m^3, than the published average sedimentary heat generation of 2.1μW/m^3 (Beardsmore & Cull 2001). Sandstones had the lowest value of all at ~1.2μW/m^3 which correlates well with a published range of 0.9-1.2μW/m^3 (Beardsmore & Cull 2001). All four Devonian granites examined in this project produced high heat generation values, 7- 10.5μW/m^3, compared to the published range for the global average for granites of 2.5-5.5μW/m^3 but are within the range of values from South Australia 4.5-61.6μW/m^3 (Matthews & Beardsmore 2007; Neumann, Sandiford & Foden 2000). The Royal George and Gipps Creek granites are S-type granites from the Ben Lomond Batholith and had the highest values, 8.2-10.5μW/m^3. The top three individual heat generation values, 11μW/m^3, 12μW/m^3 and 22μW/m^3, all came from the Royal George granite.

6.1 Future Research and Applications

Low sonic velocities and low thermal conductivities correspond to Mathinna Group shales. Low thermally conductive shales may trap heat produced by radiogenic granites. Therefore it may be possible to use regional seismic surveys to highlight areas of low sonic velocity that may be the low thermal conductivity shales. Seismic surveys are a cheaper and quicker method than drilling to determine the underlying geology and will save geothermal explorers time and money.

Further studies are also needed to determine why the shales have low thermal conductivities compared to the sandstones and siltstones. Perhaps a mineralogical analysis of quartz, feldspars and mica will reveal links for thermal conductivity and lithology. It is known that high quartz contents, particularly in sandstones, correspond to high thermal conductivities (Gunn et al. 2005).

Using Gamma Ray Spectroscopy to determine the K, U and Th content of possible heat producing granites (and sediments) is clearly a viable alternative to XRF and LA-ICP-MS. No preparation of the samples was required and they can be analysed very quickly saving time provided that a suitable lead castle is available to shield the detector from environmental gamma radiation.

7. CONCLUSION

This project was successful in using standard and developmental methods to investigate the properties of rocks in north eastern Tasmania for geothermal exploration.

Two results of this study will save geothermal explorers time and money in searching for prospective areas to drill hot geothermal resources deep underground. Utilisation of seismic surveys to pinpoint low sonic velocity areas that correspond to shale dominated sequences and therefore low thermal conductivities. And using Gamma Ray Spectroscopy, to determine the K%, U ppm and Th ppm, will minimise the cost and time of analysing rock samples to identify granites that are potential heat produces.

Areas of low thermal conductivity, shale dominated units, must be coupled with heat producing granites, of a similar composition to the Ben Lomond Batholith, to produce high temperature geothermal resources. The overlying shales act as insulators to minimise heat lost to the surface and ensure high temperatures at depth suitable to produce geothermal electricity.

ACKNOWLEDGEMENTS

The authors would like to thank KUTh Energy Ltd and the UTAS for purchasing the PEDB for this study and for providing financial support, and MRT for further scholarship support.

This research was undertaken by Hilary Goh as an Honours project for the duration of one year at the University of Tasmania. Drs. Michael Roach and Anya Reading were supervisors.

REFERENCES

Adams, JAS & Gasparini, P 1970, *Gamma-ray spectrometry of rocks*, Elsevier Publishing Company, Amsterdam.

AUA 2007, *Australia's electricity*, Australian Uranium Association Ltd, <www.uic.com.au>.

Barbier, E 2002, 'Geothermal energy technology and current status: an overview', *Renewable and Sustainable Energy Reviews*, vol. 6, pp. 3-65.

Beardsmore, GR & Cull, JP 2001, *Crustal heat flow: a guide to measurement and modelling*, Cambridge University Press, Cambridge, United Kingdom.

Bottrill, RS, Brown, AV, Calver, CR, Corbett, KD, Green, GR, McClenaghan, MP, Pemburton, J, Seymour, DB & Taheri, J 1998, 'A summary of the economic geology and mineral potential of Late Proterozoic and Palaeozoic provinces in Tasmania', *Journal of Australian Geology and Geophysics*, vol. 17, no. 3, pp. 123-143.

Burrett, CF & Martin, EL 1989, *Geology and mineral resources of Tasmania, Special publication 15*, vol. Special publication 15, Geological Society of Australia.

Fridleifsson, IB, Bertani, R, Huenges, E, Lund, JW, Ragnarsson, A & Rybach, L 2008, *The possible role and contribution of geothermal energy to the mitigation of climate change*, Intergovernmental Panel on Climate Change, Germany.

Gunn, DA, Jones, LD, Raines, MG, Entwisle, DC & Hobbs, PRN 2005, 'Laboratory measurement and correction of thermal properties for application to the rock mass', *Geotechnical and Geological Engineering*, vol. 23, no. 6, pp. 773-791.

IAEA 1991, 'Airborne gamma ray spectrometer surveying.' *International Atomic Energy Agency, Technical Report Series*, vol. 323.

Leaman, DE 1994, 'The Tamar Fracture System in Australia: Does it exist?' *Australian Journal of Earth Sciences*, vol. 41, pp. 73-74.

Matthews, C & Beardsmore, G 2007, 'New heat flow data from south-eastern South Australia', *Exploration Geophysics*, vol. 38, pp. 260-269.

McClenaghan, MP 2006, *The geochemistry of Tasmanian Devonian-Carboniferous granites and implications for the composition of their source rocks*, Mineral Resources Tasmania, viewed.

Minty, BRS, Luyendyk, AJP & Brodie, RC 1997, 'Calibration and data processing for airborne gamma-ray spectrometry', *AGSO Journal of Australian Geology & Geophysics*, vol. 17, no. 2, pp. 51-62.

Neumann, N, Sandiford, M & Foden, J 2000, 'Regional geochemistry and continental heat flow: implications for the origin of the South Australian heat flow anomaly', *Earth and Planetary Science Letters*, vol. 183, no. 1-2, pp. 107-120.

Popov, Y, Tertychnyi, V, Romushkevich, R, Korobkov, D & Pohl, J 2003, 'Interrelations between thermal conductivity and other physical properties of rocks: Experimental data', *Pure and Applied Geophysics*, vol. 160, no. 5-6, pp. 1137-1161.

Powell, CM, Baillie, PW, Conaghan, PJ & Turner, NJ 1993, 'The mid-Palaeozoic turbiditic Mathinna Group, northeast Tasmania', *Australian Journal of Earth Sciences*, vol. 40, pp. 169-196.

Seymour, DB, Green, GR & Calver, CR 2007, *Tasmania Surface Geology*, Geological Survey Bulletin 72.

Surma, F & Geraud, Y 2003, 'Porosity and Thermal Conductivity of the Soultz-sous-Foreˆts Granite', *Pure and Applied Geophysics*, vol. 160, pp. 1125-1136.

Telford, WM, Geldart, LP & Sheriff, RE 1990, *Applied Geophysics*, Second edn, Cambridge University Press, Cambridge.

Zumdahl, SS 2000, *Introductory chemistry: a foundation*, Fourth edn, Houghton Mifflin, Boston.

Web sources

www.matweb.com/index.aspx

Table 3: Mean values are given for each lithology excluding outliers where indicated in the table. Heat production is broken into individual plutonic sources. Electrical resistivities are highly variable therefore median values are displayed in this table.

	North east Tasmanian rock properties, mean values									
	Lithology/ pluton	**No. of samples**	**Heat prod. $\mu W/m^3$**	**Mag sus. $x10^{-3}$**	**Dry density g/cm^3**	**Wet density g/cm^3**	**Porosity %**	**Sonic velocity km/s**	**Elect res. $\Omega m, x10^4$ #**	**Thermal cond. W/mk**
Mathinna Group		**58**	**1.61 ±0.03**							
	Sandstones	24	1.20 ±0.03	0.06*	2.69*	2.69*	0.41*	5.35*	1.20	4.48 ±0.22*
	Siltstones and mudstone	16	1.87 ±0.05	0.40	2.76	2.76	0.56	5.18	1.30	3.33 ±0.14*
	Shales	18	1.93 ±0.04	0.16	2.77	2.76	0.70*	4.29	1.70	2.70 ±0.10*
Devonian granite		**31**	**8.13 ±0.23**	**0.03**	**2.58**	**2.60**	**0.56**	**5.49**	**1.30**	**3.48 ±0.15***
	Poimena	6	7.17 ±0.28							
	Gipps Creek	4	8.23 ±0.41*							
	Royal George	14	10.51 ±0.24							
	Coles Bay	7	7.33 0.17							

* excluding outliers, # median values